

ETH SEMESTER PROJECT

# THE FORMATION OF STELLAR CLUSTERS AT HIGH REDSHIFTS IN COSMOLOGICAL SIMULATIONS

Mila Luescher

Prof. Dr. Robert Feldmann

Prof. Dr. Lavinia Heisenberg

Dr. Luigi Bassini

February 16, 2022

## Abstract

This report discusses the formation and evolution of globular clusters in three high redshift ( $z \geq 6.0$ ) galaxies. After identifying the globular clusters in the galaxies, their mass- and luminosity-functions are evaluated and discussed. Furthermore, the relation between the number of globular clusters and the halo mass is tested. The impact of the simulation mass-resolution as well as different feedback models is also examined. Finally, the formation sites of the the globular clusters are determined.

It was found that the mass function of the clusters follows a power-law shape with a slope close to, but below, the theoretical value of  $\beta \approx 2$ . On the other hand, the luminosity function followed a log-normal shape. Increasing the resolution of the simulation solely adds clusters at lower masses, without changing the shape of the mass function. Feedback, especially from supernovae, largely reduces the number of low-mass young clusters in a galaxy. Finally, it was found that stellar clusters form in regions of high density near the centre of the galaxy and later disperse.

# Contents

<b>1</b>	<b>Introduction</b>	<b>3</b>
<b>2</b>	<b>Theory &amp; Observations</b>	<b>3</b>
2.1	Mass and Luminosity Function . . . . .	4
2.2	The Number of Globular Clusters . . . . .	5
<b>3</b>	<b>Simulations</b>	<b>6</b>
3.1	GIZMO . . . . .	6
3.2	FIRE Project . . . . .	7
3.3	Cosmological Zoom-in Simulations . . . . .	8
<b>4</b>	<b>Analysis</b>	<b>9</b>
4.1	Analysis Tools: PHINDER & FIREStudio . . . . .	9
4.2	Cluster Mass Function . . . . .	9
4.3	Cluster Luminosity Function . . . . .	12
4.4	HR vs. VHR . . . . .	13
4.5	Number of Clusters vs. Halo Mass . . . . .	13
4.6	The Impact of Feedback . . . . .	15
4.7	Where do the Globular Clusters form? . . . . .	17
<b>5</b>	<b>Conclusion</b>	<b>18</b>
	<b>Bibliography</b>	<b>19</b>

# 1 Introduction

It is a natural curiosity to want to know how our universe formed and what rules it is governed by. One of the most fundamental questions involves the formation of galaxies, stars, and other astrophysical bodies. In this semester project we scratch the surface of one of these questions: *how did globular clusters form?* A lot has already been discovered about globular clusters by looking at nearby galaxies but observationally resolving globular clusters in high redshift galaxies is increasingly more difficult. The goal of this semester project was to use the power of computational astrophysics to identify and analyse globular clusters in high redshift galaxies, simulated with the code GIZMO(Philip F. Hopkins 2015) and FIRE-physics(Philip F. Hopkins et al. 2014).

After introducing some of the theory relevant to this report, I will outline the simulations used to create the galaxies. In a next section I discuss the analysis done on the simulated galaxies. After identifying the clusters in the galaxy we took a look at their mass and luminosity functions as well as how the total number of clusters relates to the galaxies halo mass. The impact of feedback and resolution on the simulations is also investigated. Lastly, we will investigate where in the galaxy the clusters are formed and where they move as they age. In the last section I will briefly summarise the results found as well as how they can be improved through further work.

# 2 Theory & Observations

As the word already suggests, globular clusters (GC) are a tightly bound, spherical collection of stars, which usually reside in the halo of their host galaxy (see Figure 1 (NASA, ESA, and Feild(STScl) 2019)). Traditionally, globular clusters are characterised by the amount of stars ( $\sim 10^4 - 10^6$ ), their mass ( $\sim 10^4 - 10^6 M_{\odot}$ ) or their old age. They are generally depleted of any gas or dust and exhibit no young stars, which supports the idea that they formed together with their host galaxy. In addition, the stars in the globular clusters all have similar metallicity which suggests that they are of similar age. All this was found by looking at our galaxy, the Milky Way, as well as nearby galaxies, such as M31, and thus characterises only the old globular clusters. We want to take a closer look at how globular clusters formed and how their characteristics at young ages might differ from what we know to be true about them today.



Figure 1: An artists depiction of the Milky Way, its bulge, disk and its globular clusters.

The progenitors to globular clusters are thought to be young massive clusters (YMC) which usually have masses ranging between  $10^4 - 10^8 M_{\odot}$ . YMC have been observed in high-pressure regions of nearby galaxies (although it is unclear if they could still evolve into globular clusters at low redshifts) and in galaxy mergers. Since galaxies at high redshifts

are very turbulent and subject to frequent mergers, they are also a breeding ground for YMC.

Kruijssen 2015 proposed a 2-phase GC formation model in which the YMC are thought to form in the disk of high-redshift galaxies and subsequently are moved into the galaxy halo through a merger event. Once the YMC are formed they frequently are disrupted by giant molecular clouds. As described by Kruijssen 2012 the mass-loss rate for YMC in the first phase of their life is given by

$$\left( \frac{dM}{dt} \right)_{\text{cce}} = -\frac{M}{t_{\text{cce}}} \quad (1)$$

$$t_{\text{cce}} = t_{5,\text{cce}} \left( \frac{f_{\Sigma}}{4} \right)^{-1} \left( \frac{\rho_{\text{ISM}}}{M_{\odot} \text{pc}^{-3}} \right)^{-3/2} \cdot \left( \frac{M}{10^5 M_{\odot}} \right) \phi_{\text{ad}}^{-1} \quad (2)$$

where  $t_{\text{cce}}$  is the disruption timescale ('cce' meaning 'cruel cradle effect'),  $t_{5,\text{cce}} = 176 \text{ Myr}$  is the proportionality constant and  $f_{\Sigma}$  is the giant-molecular-cloud surface density to mean gas surface density ratio. We can see, since the disruption time scale is a lot shorter than the age of the universe, that these YMC will only evolve into surviving globular clusters if they leave the disk. Anything from tidal heating to major/minor mergers can cause YMC to be ejected out of the galactic disc and into the halo. In the case of minor mergers, migration happens via violent relaxation, whereas for major mergers the driving factor is tidal stripping. Once the YMC have managed to leave the turbulent environment of the galactic disk, the only mass-loss will be through evaporation

$$\left( \frac{dM}{dt} \right)_{\text{evap}} = -\frac{M}{t_{\text{evap}}} \quad (3)$$

$$t_{\text{evap}} = t_{5,\text{evap}} \left( \frac{M}{10^5 M_{\odot}} \right)^{\gamma} \quad (4)$$

where the disruption timescale can range up to 100Gyrs, which allows the globular clusters to survive until today.

## 2.1 Mass and Luminosity Function

As the globular clusters evolve over time, so does their mass function. Generally the mass function of young massive clusters (or cluster initial mass function CIMF) can be described by Schechter distribution (Schechter 1976, discussed in Portegies Zwart, McMillan, and Gieles 2010)

$$\phi(M) \equiv \frac{dN}{dM} = AM^{-\beta} e^{-M/M_{\star}} \quad (5)$$

where  $\beta \approx 2$  and  $M_{\star}$  is the Schechter mass that characterises the truncation. The Schechter mass can take on different values depending on how quiescent, or turbulent the galaxy in question is. For the analysis here, we will be using a simplified model where we define the mass function to peak at around  $10^5 M_{\odot}$  and drop off.

$$\phi(M) \equiv \frac{dN}{dM} \propto M^{-\beta} \quad (6)$$

As times goes on, more and more of the low mass globular clusters fully evaporate. This leads to the currently observed globular cluster mass function (GCMF) to be more log-normally shaped.

Similar to the mass function, the luminosity function can also be described by a power law. Whitmore et al. 1999 found that the globular clusters luminosity function can be described as followed

$$\phi(L) \equiv \frac{dN}{dL} \propto L^{-\alpha} \quad (7)$$

where  $\alpha \approx 2$ . The data is based on observations of luminous point sources in the Antennae galaxy. Even though the Antennae galaxy is not a high-redshift galaxy it still exhibits many YMC since it is currently going through a starburst phase triggered by a merger event. Galaxies which exhibit little starburst (such as the Milky Way), and thus mostly host old globular clusters, tend to have GC with a luminosity function in a log-normal shape.

## 2.2 The Number of Globular Clusters

Another characteristic of globular clusters is the amount present in a galaxy. Burkert and Forbes 2020 analysed observational data of multiple galaxies and found a correlation between the number of globular clusters in a galaxy and the galaxies dark matter halo mass.

$$\begin{aligned} \langle \log N_{GC} \rangle &= -9.58(\pm 1.58) \\ &+ 0.99(\pm 0.13) \times \log \frac{M_{\text{vir}}}{M_\odot} \end{aligned} \quad (8)$$

It needs to be noted, that the observational data used was from low-redshift galaxies and thus the luminosity function of the globular clusters had a log-normal shape. They estimated the number of globular clusters by assuming the luminosity function to be symmetric and doubling the number of globular clusters to the right of the peak. This result corresponds on average to about one globular clusters per  $5 \times 10^9 M_\odot$  dark matter halo mass.

### 3 Simulations

The data used for this project, was taken from multiple cosmological zoom-in simulations performed with the massively-parallel and multi-physics simulations code GIZMO, using the physics from FIRE-2<sup>1</sup>.

#### 3.1 GIZMO

The code GIZMO (Philip F. Hopkins 2015) is a heavily modified version of GADGET-3 (Springel, Yoshida, and White 2001), which is an  $N$ -body smoothed particle hydrodynamics code for cosmological simulations. The goal of GIZMO was to find a good middle-ground between adaptive mesh refinement (AMR) and smoothed-particle hydrodynamics (SPH), by solving the fluid equations with a new Lagrangian Godunov solver. This new method uses a moving particle distribution which automatically adapts to the resolution of the area. By doing so, it also avoids certain issues that come with SPH or AMR. Other than most codes, it allows the user to choose which hydrodynamics solver the code should use: Either the new Lagrangian methods (Meshless Finite-Mass or Meshless Finite-Volume), regular SPH, regular AMR, or a moving Voronoi-type mesh. Some examples of the different mesh structures are shown in Figure 2<sup>2</sup>

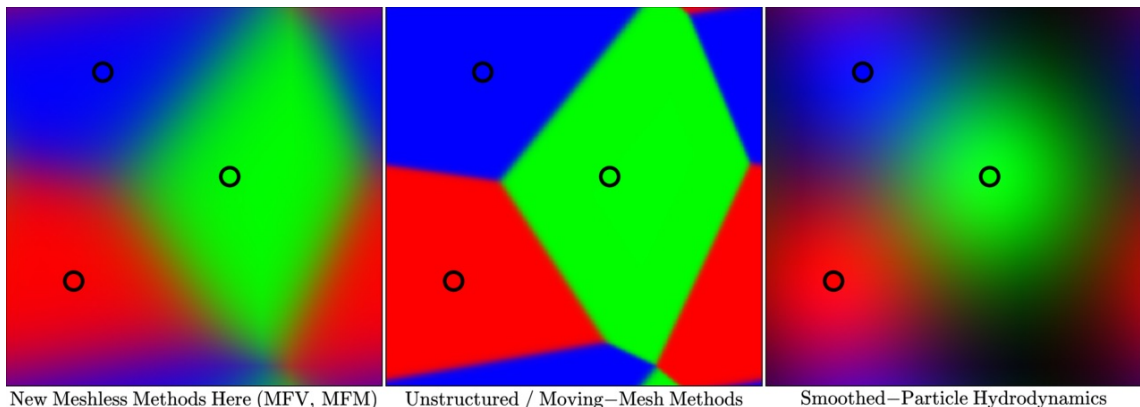


Figure 2: A depiction of three different mesh geometries available in the GIZMO code. The structure of the meshless method is visualised in the left image and uses smooth edges. On the other hand, the unstructured/moving-mesh methods use a grid which has boundaries with step functions at the edges. On the right is an image of the meshless SPH method.

For the simulations used in this project a meshless finite-mass Lagrangian Godunov method was used, which provides adaptive spatial resolution as well as conservation of energy, mass and momentum. This method assures that each particle has a fixed mass by allowing the faces between particles to deform, such that there is no mass flux between the particles. Choosing this solver also confines us to one particular mesh-motion, the Lagrangian mesh (Figure 3<sup>3</sup>). This means that the mesh moves with the mean fluid motion, once again making sure that the masses stay fixed.

In addition, if the solver allows it, the user may also choose what type of motion their mesh should have, i.e an expanding/outflowing mesh, a differentially rotating mesh, etc. This is different from the geometry of the mesh and purely describes how the mesh moves over time.

<sup>1</sup><https://fire.northwestern.edu>

<sup>2</sup>Image taken from the GIZMO user guide [http://www.tapir.caltech.edu/~phopkins/Site/GIZMO\\_files/gizmo\\_documentation.html#hydro](http://www.tapir.caltech.edu/~phopkins/Site/GIZMO_files/gizmo_documentation.html#hydro)

<sup>3</sup>Image taken from the GIZMO user guide [http://www.tapir.caltech.edu/~phopkins/Site/GIZMO\\_files/gizmo\\_documentation.html#hydro](http://www.tapir.caltech.edu/~phopkins/Site/GIZMO_files/gizmo_documentation.html#hydro)

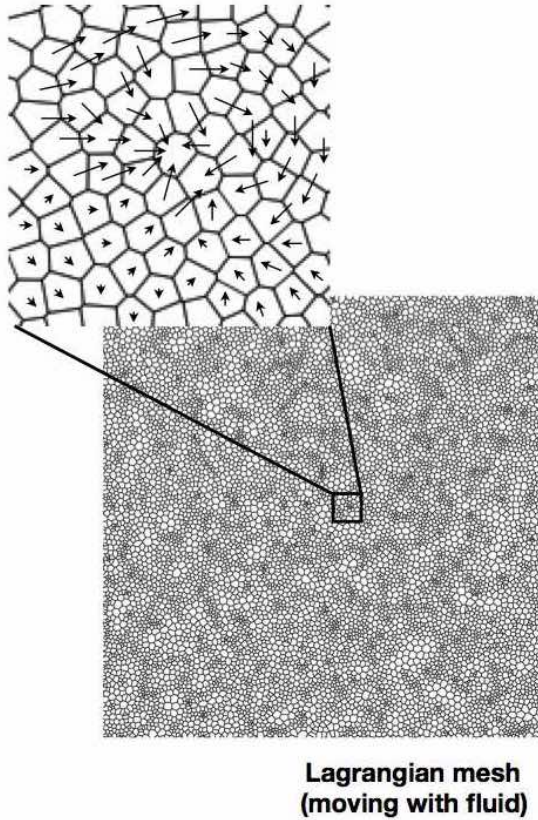


Figure 3: A depiction of the mesh-motion used in our simulations. Such a mesh is called a Lagrangian mesh and moves with the fluid, while keeping the mass per particle constant.

Even though GIZMO has a large variety of physical modules to choose from, these were not utilised for these simulations. Instead, the physics was simulated with the FIRE-2 model.

### 3.2 FIRE Project

The FIRE (Feedback In Realistic Environments) project (Philip F. Hopkins et al. 2014) is a large scale collaboration that aims at simulating feedback more realistically. Compared to the resolution of cosmological (zoom-in) simulations, the size of a star is barely a speck of dust. Thus, is it nearly impossible to resolve stars fully and so called sub-grid (sub-resolution) models need to be implemented, in order to model stellar physics. As expected, sub-grid models are only accurate up to a certain level since they tend to simplify physical processes which in reality are highly complex. FIRE aims at circumventing this issue by resolving the main players in star formation and stellar feedback. For example, FIRE resolves the formation of giant molecular clouds (GMC) as well as the interstellar medium (ISM). In addition, it takes into account the energy, momentum, metals, and mass returned from stars through feedback. By doing so they account for stellar feedback from radiation pressure, photo-ionisation and photo-electric heating, stellar winds and supernovae type I and II (more feedback models such as AGN are in process). All this allows for a treatment of stellar evolution in a cosmological context.

The galaxies used in this project were simulated with FIRE-2 physics implemented into the GIZMO code. FIRE-2 (Philip F Hopkins et al. 2018) is an update version of FIRE(-1) and uses MFM instead of its predecessors “pressure-energy” variant of smoothed-particle hydrodynamics (P-SPH).

### 3.3 Cosmological Zoom-in Simulations

Cosmological simulations are frequently used to test cosmological models, the one most consistent with observations is the  $\Lambda$ CDM model. When wanting to study smaller structures, such as galaxy clusters, or even singular galaxies, it becomes incredibly expensive and time consuming to simulate such a large box-size (usually within  $10 - 100 \text{ Mpc } h^{-1}$ ) with large enough resolution to see the structures of a galaxy. Due to this, zoom-in cosmological simulations are often used instead. Here, a large 'box' of the universe is first simulated on a coarse level for a certain cosmological model and initial conditions. Once completed, a target dark matter halo is selected and new initial conditions are generated for a smaller box (usually with box-length 0.001 times smaller) encapsulating the halo. This dark matter halo is then re-simulated on a finer level and with the new initial conditions. Such cosmological zoom-in simulations were also used for the galaxies in this project.

## 4 Analysis

In this chapter, I would like to present the analysis done on the simulations and discuss their outcomes. The three key aspects investigated were the mass and luminosity function of the globular clusters as well as the number of globular clusters as a function of halo mass. Furthermore, we looked at how the resolution of the simulation and feedback influence the results. Finally, we also took a brief look at where the globular clusters form and where they move after.

### 4.1 Analysis Tools: PHINDER & FIREStudio

Before any analysis on the globular clusters could be done, we first needed to identify them. Following the work done by Ma et al. 2020 we used the python package PHINDER<sup>4</sup> to identify the potential wells of stars in our simulations. By doing so, PHINDER found both the bound and unbound clusters with a minimum of 32 stellar particles. For our use, only the bound clusters were of importance. While identifying the clusters, PHINDER also creates a data file which contains the location, mass and half-mass radius of the clusters as well as the number of particles the clusters consist of.

Since the code was created for isolated galaxies, we needed to adjust it slightly before use to account for cosmological simulations. In addition, for the calculation of the potential we added a slight 'softening'  $s$  to avoid singularities. This means, that in calculating the gravitational potential between two particles, the potential scales like

$$\Phi \propto -\frac{1}{\sqrt{r^2 + s^2}} \quad (9)$$

instead of  $\propto -1/r$ , and hence prevents the potential from going to infinity when the particles get too close to each other. Nevertheless, the softening parameter should still be chosen very small, in order to keep the simulations realistic. For our purpose we chose a softening parameter of  $s = 0.0043$ .

After running the cluster finder on our simulations we discarded all clusters large than 100pc and outside  $R_{\text{vir}}$  of the galactic center. In Figure 4 one can see the remaining bound stellar clusters overlapped on a 'true color' rendering of the three galaxies B400-02,-10 and -17 over different redshifts. In B400 02 one can see that there is a large amount of clusters near the center of the galaxy in addition to there being many globular clusters in the galaxy halo. Later we will analyse if these clusters were born in the halo, or if they migrated there. Figure 5 shows the globular clusters overlapped on a more zoomed-in stellar density map. Here one can see the clusters more clearly by eye and assures us that we are correctly identifying the globular clusters.

The images over which we plotted the globular clusters (shown in Figure 4) were made with FIRE-Studio<sup>5</sup>, a python visualisation package created for the FIRE-simulations. It takes into account the light from stars as well as the light absorbed by dust particles, resulting in an image close to what would observationally be detected. In addition to the image, FIRE-Studio also outputs a file with the luminosity of each pixel. It does this for the SDSS (Sloan Digital Sky Survey) filters  $u$  (ultraviolet,  $\lambda_u = 3551.0 \text{ \AA}$ ),  $g$  (green,  $\lambda_g = 4686.0 \text{ \AA}$ ) and  $r$  (red,  $\lambda_r = 6165.0 \text{ \AA}$ ). This will later be useful for probing the luminosity function of the globular clusters.

### 4.2 Cluster Mass Function

A next step was to identify the mass function of the clusters for the three different galaxies (B400-10, -17 and -02) at three redshifts  $z = 8.0, 6.0, 7.0$ . The masses of the clusters were

<sup>4</sup>Code available at <https://github.com/mikegrudic/Phinder>

<sup>5</sup>Code available at [https://github.com/agurvich/FIRE\\_studio](https://github.com/agurvich/FIRE_studio)

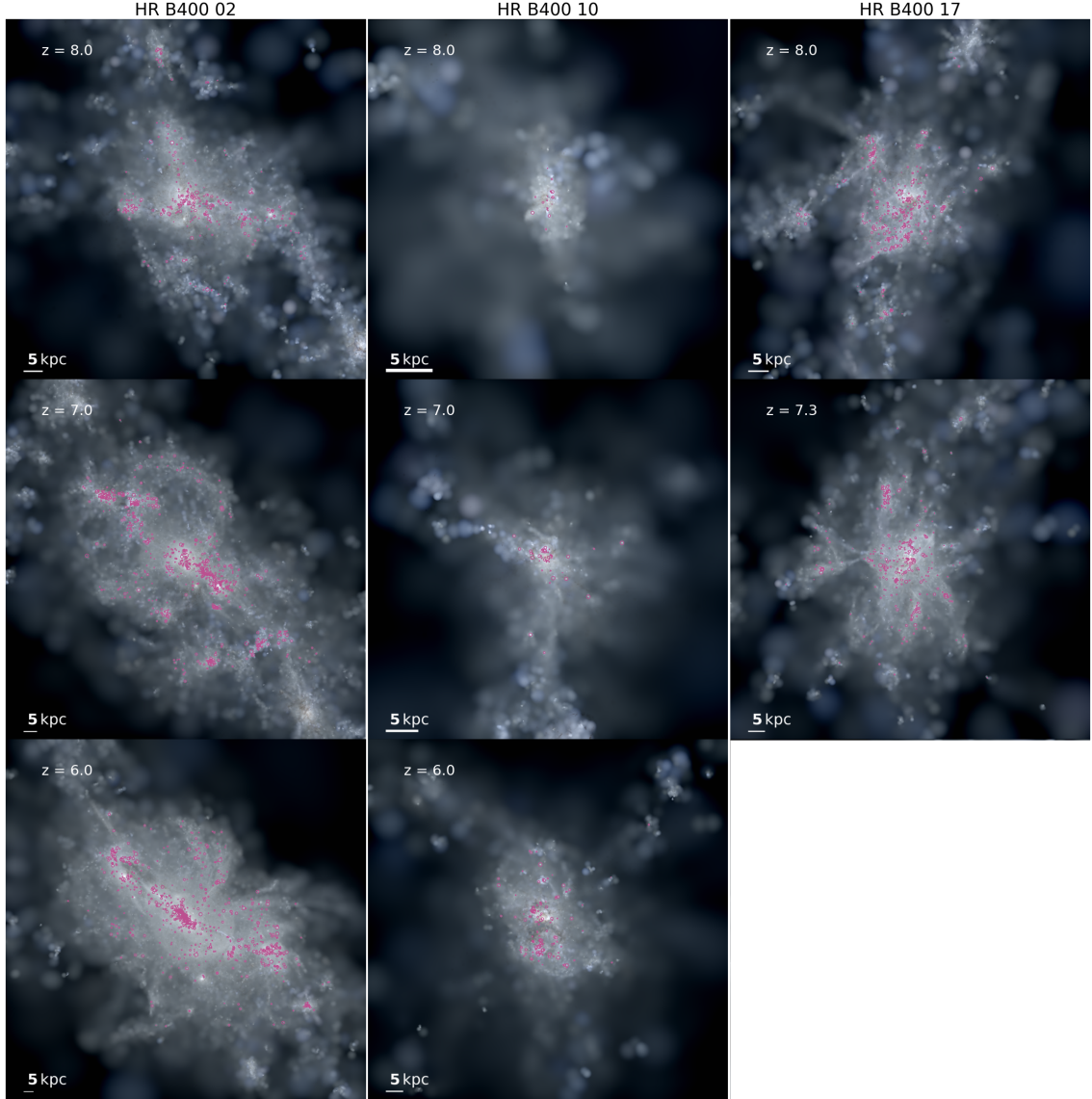


Figure 4: A mock-observation image of three galaxies at different redshifts. The circles visualise the globular clusters. B400 17 was only run until redshift  $z = 7.3$ , due to long simulation times.

taken from the data file created by PHINDER. In order to productively compare the mass functions of the different galaxies we used the number of clusters per galaxy  $N_{\text{tot}}$  as a normalisation factor. After plotting the mass function logarithmically (Figure 6), a linear least-squares fit was performed on it to find the slope  $\beta$  corresponding to Equation 6. The values for both  $N_{\text{tot}}$  and  $\beta$  can be found in Table 1. As expected the mass functions take on a power-law shape. The slopes are all below but close to the theoretical value of  $\beta \approx 2$ . This also agrees with the results found by Ma et al. 2020 which also investigated the mass function of newly formed globular clusters from simulations. It needs to be noted, that compared to the other simulations B400-10 is not following the power-law as nicely. This is to be expected though, since B400-10 is a small galaxy and does not have many globular clusters, leading to the large fluctuations in the mass function.

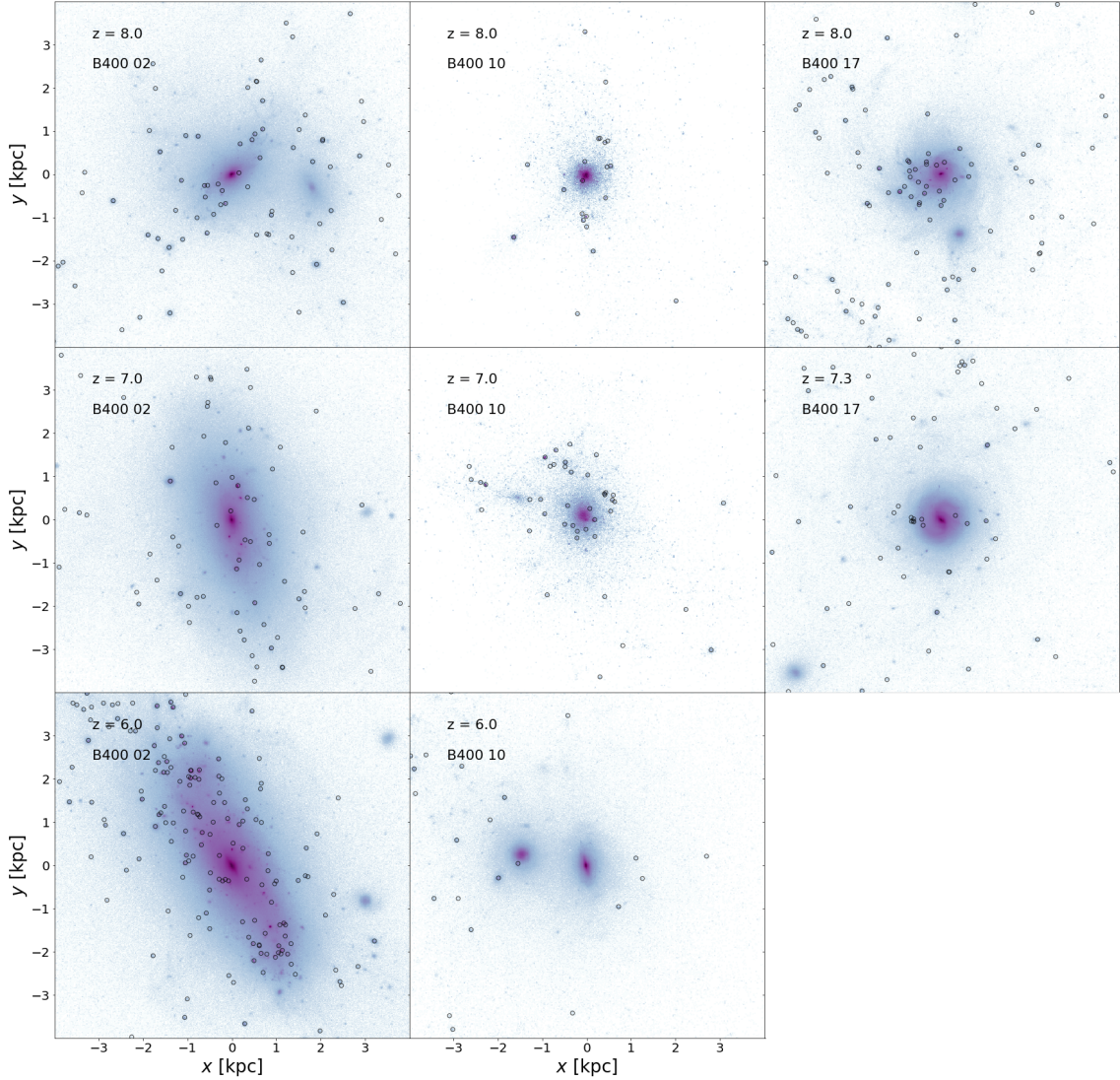


Figure 5: Stellar densities overlapped by the stellar clusters (black circles) for the three simulation B400-02, -10 and -17 at redshifts  $z = 8.0, 7.0, 6.0$  within 3kpc of the center.

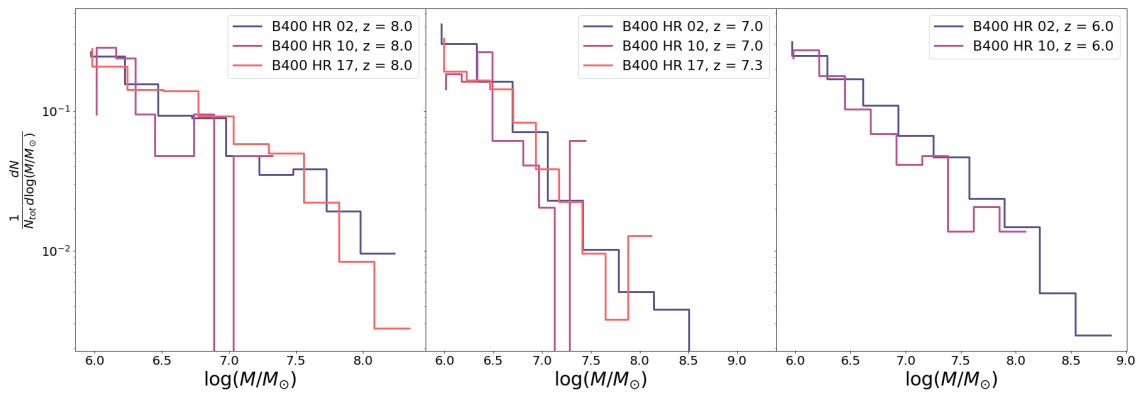


Figure 6: The mass function for three different galaxies B400-02, -10 and -17 at redshifts  $z = 8.0, 7.0, 6.0$ , with the number of clusters per galaxy  $N_{\text{tot}}$  used for normalisation.

	B400-02			B400-10			B400-17	
$z$	8.0 313	7.0 788	6.0 809	8.0 21	7.0 49	6.0 146	8.0 360	7.3 313
$\beta$	$1.6 \pm 0.1$	$1.8 \pm 0.1$	$1.7 \pm 0.1$	$1.5 \pm 0.2$	$1.6 \pm 0.2$	$1.7 \pm 0.1$	$1.8 \pm 0.1$	$1.9 \pm 0.1$

Table 1: The number of globular clusters per galaxy  $N_{\text{tot}}$  as well as the fitted slope  $\beta$  are given for three galaxies at different redshifts.

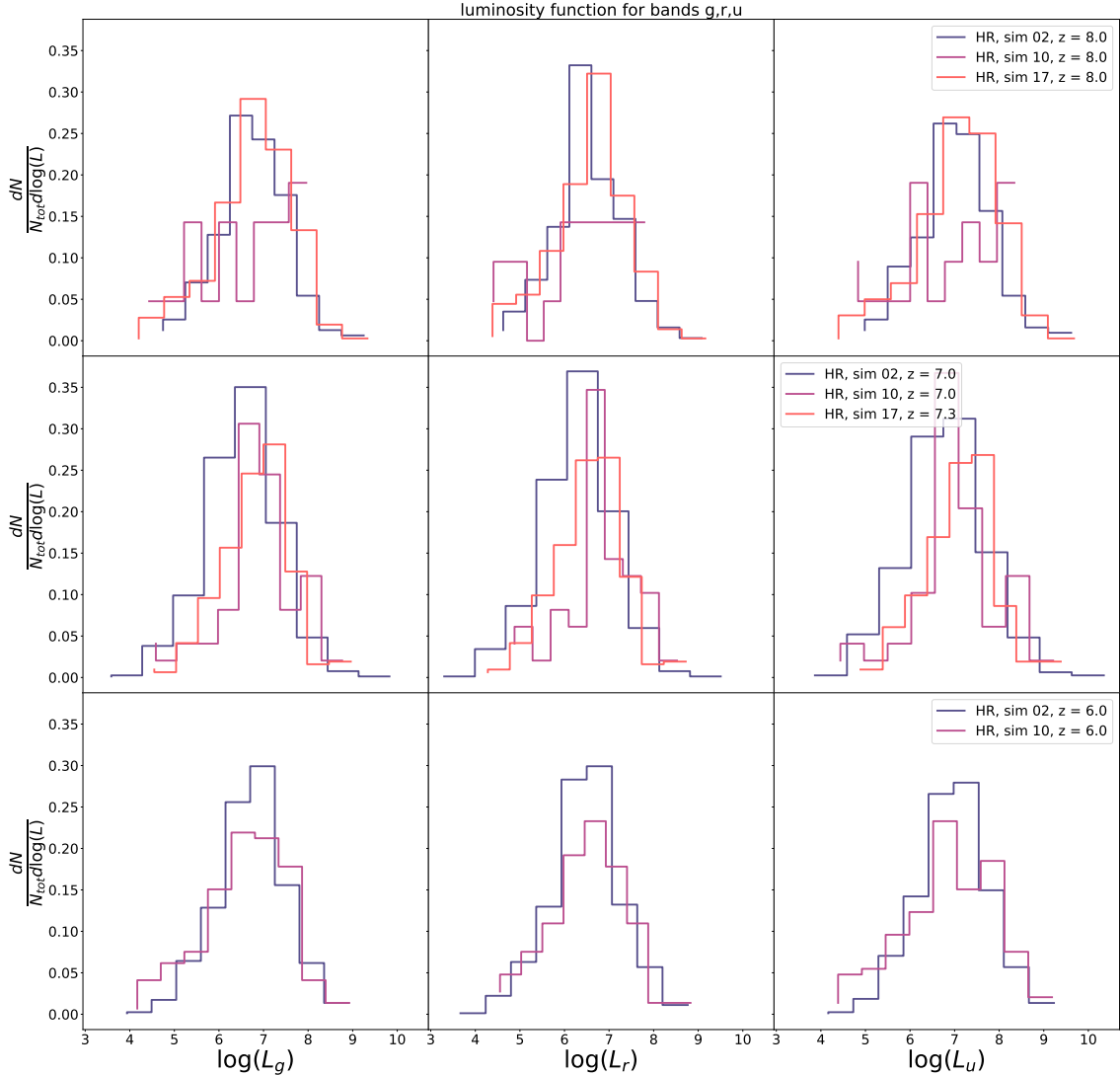


Figure 7: Above one can see the luminosity functions for the three galaxies B400-02, -10 and-17 over redshifts  $z = 8.0, 7.0, 6.0$  and for three different bands  $u, r$  and  $g$ .

### 4.3 Cluster Luminosity Function

In order to probe the luminosity function of the globular clusters we made use of the images created by FIRE-Studio, which also output the luminosity per pixel. First, we rescaled the coordinates of the globular clusters to match the image-size. Then, all the pixels within (or overlapping) the half-mass radius of the globular clusters were chosen and the luminosities added up. This resulted in the luminosity functions seen in Figure 7. Surprisingly, the luminosity function does not look like a power-law but has more of a log-normal shape. It is still unclear to us why we see this shape for YMC here but we have a few suspicions about our calculations. Since we take all pixels that overlap the half-mass radius we might be over-estimating the luminosity of the clusters and thus might be biased towards low-

luminosity clusters. The fact that the luminosities taken from FIRE-Studio account for dust attenuation might also have an impact on the shape of the luminosity function. Another concern was the resolution chosen for the pixels. We tested how the luminosity function changes for three different pixel resolutions 45, 30 and 15pc. As we can see in Figure 8 the resolution did not change the shape of the luminosity function significantly. In the end we chose a resolution of 30pc since 15pc is too close to the softening of the stars ( $\approx 4$ pc) and 45pc is already a lot larger than the half-mass radii of most of the clusters. All in all, further investigation of the luminosity function is needed and it would be advantageous to compute the luminosity of each globular cluster from scratch.

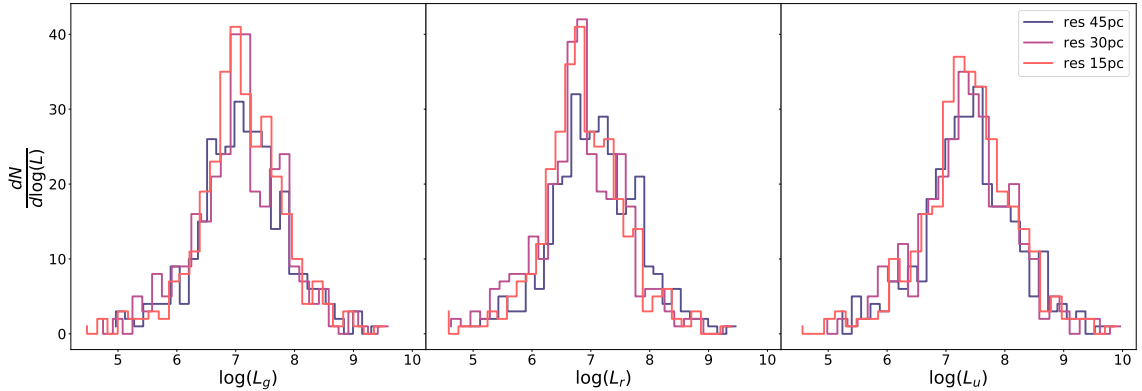


Figure 8: Luminosity function for the galaxy B400-02 at redshift  $z = 8.0$  for three different resolutions (45,30 and 15pc)

#### 4.4 HR vs. VHR

It was also important to check how our results change if we increase the mass resolution of the simulations. Up until now all galaxies were simulated with high resolution (HR) which means each stellar particle has a mass of about  $\approx 3.6 \times 10^4 M_{\odot}$ . This means that, since PHINDER has a lower limit of 32 particles per bound cluster, the lower mass limit for the globular clusters is around  $\approx 10^6 M_{\odot}$ . Changing the resolution from HR to VHR (very high resolution) decreases the globular cluster mass limit to  $\approx 4.5 \times 10^3 M_{\odot}$  which allows for the lightest GC to be  $\approx 10^5 M_{\odot}$ .

Due to the shape of the mass function, one would expect for this additional range of cluster masses to unveil a lot of globular clusters which were previously left undetected. As one can see in Figure 9, especially B400-17 VHR added many more globular clusters than B400-17 HR. The increase in B400-10 does not seem as large, but the percentile increase is still substantial.

When looking at the mass functions (Figure 10), we can see that for B400-17 the VHR and HR (non-normalised) mass function follow the same line and VHR seems to just fill in the additional lower mass range. This tells us, that the choice of resolution does not change the shape of the mass function but purely informs the mass-range of available data. In other words, increasing the resolution does not seem to affect the globular clusters identified at lower resolutions. B400-10 at  $z = 6.0$  contradicts this, since the HR simulation does not overlap with the VHR simulation. Once again, this could be due to B400-10 HR not having enough clusters to fully resolve the shape of the mass function.

#### 4.5 Number of Clusters vs. Halo Mass

A next step was to evaluate if the number of globular clusters relates to the galaxies halo mass. As we can see in Figure 8 the HR data almost perfectly follows Equation 8, but

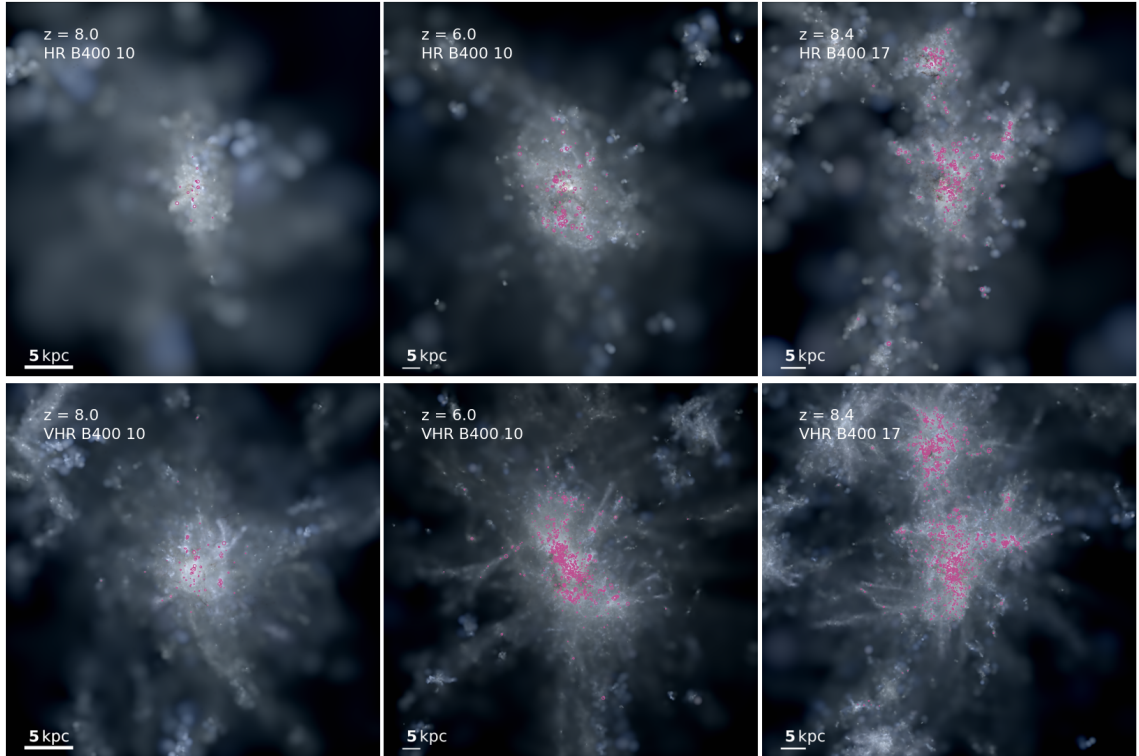


Figure 9: A mock-observation image of the galaxies B400-10 and B400-17 as well as its globular clusters, once simulated in HR and once in VHR.

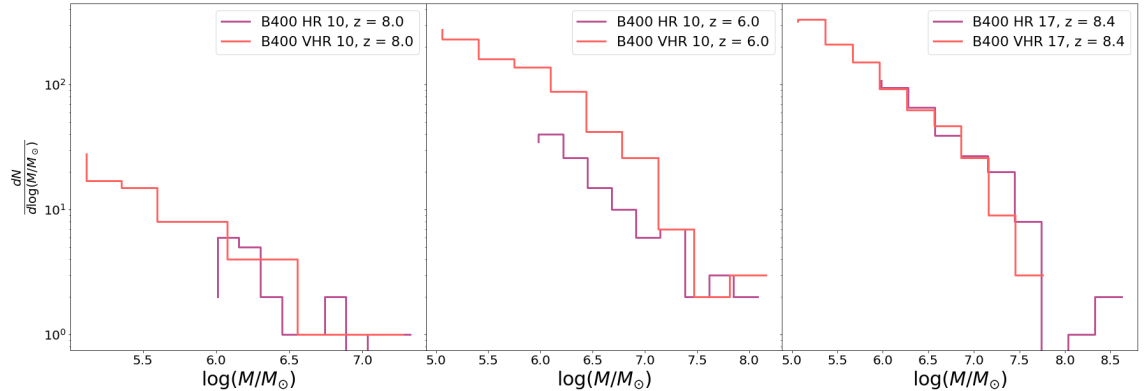


Figure 10: The mass function for B400-10 and B400-17, comparing high-resolution (HR) to very high-resolution (VHR). In order to compare the two adequately the mass functions were not normalised by the total number of clusters per galaxy  $N_{\text{tot}}$ .

	B400-10				B400-17	
Resolution	HR	VHR	HR	VHR	HR	VHR
$z$	8.0	8.0	6.0	6.0	8.4	8.4
$N_{\text{tot}}$	21	87	146	976	366	1255
$\beta$	$1.5 \pm 0.2$	$1.7 \pm 0.1$	$1.7 \pm 0.1$	$1.7 \pm 0.1$	$1.8 \pm 0.1$	$1.7 \pm 0.1$

Table 2: The number of globular clusters per galaxy  $N_{\text{tot}}$  as well as the fitted slope  $\beta$  are given for three galaxies at different redshifts.

once we take a look at the clusters from the VHR simulations this no longer holds. As we

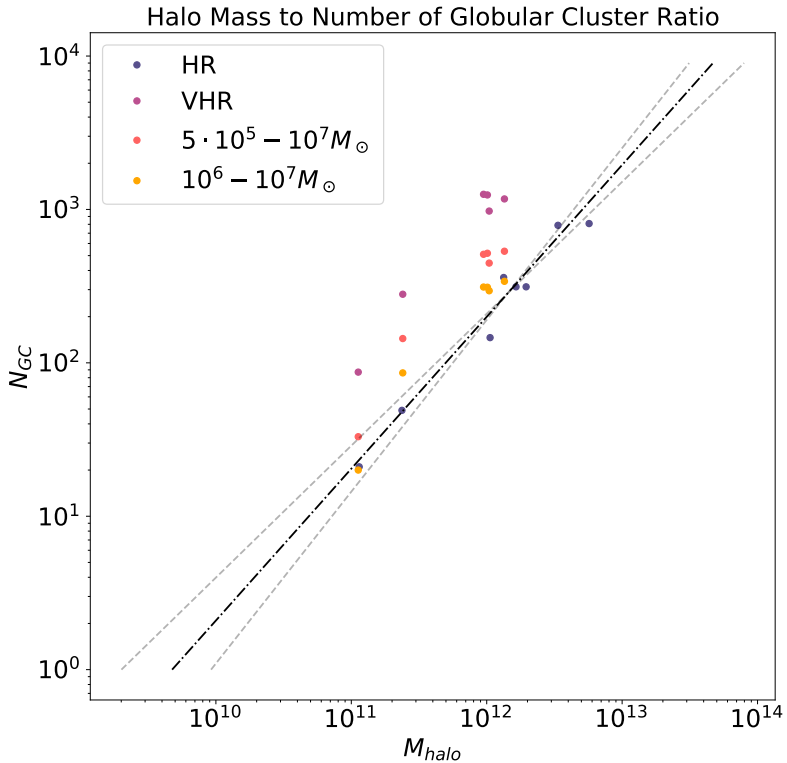


Figure 11: The number of globular clusters versus the halo mass of the galaxy. Each dot represents a galaxy at a specific redshift. The black dashed line represents the observationally found relation, stated in Equation (8), and the grey lines show its error bounds. Both HR and VHR data is displayed, as well as VHR data bound to two mass ranges ( $5 \cdot 10^5 - 10^7 M_\odot$  and  $10^6 - 10^7 M_\odot$ )

have seen, increasing the resolution of the simulation also increases the number of globular clusters by a large amount, while keeping the halo mass more or less fixed. This results in our data points being shifted upwards. Thus, it is important to know for what mass resolution the equation we are using is valid. The observational data Burkert and Forbes 2020 used to derive Equation 8 was taken from Spitzer, Forbes, and Beasley 2008. Their data covers a mass range of  $\sim 5 \times 10^5$  to  $10^7 M_\odot$ . Implementing this mass cut to the VHR simulations already brings the data points closer to the observational mean, but still not close enough.

There are a multitude of possible reasons why our mass-cut VHR data points are not following the observational data. One possibility is, that PHINDER is miss-identifying some clusters. Another reason could be, that the Spitzer data has not captured all clusters this mass range, due to some being on the same line-of-sight or otherwise covered. Additionally, we are dealing with galaxies at much higher redshifts, than the Spitzer data covers. Thus, it could be that the relation does not hold for young globular clusters, or for galaxies in the midst of their formation. Further investigation needs to be done to test these hypothesis, such as finding an alternative way of identifying the clusters and comparing it to the clusters found by PHINDER.

#### 4.6 The Impact of Feedback

Another interest of ours, was to test how different feedback models affected the globular clusters. In order to do so, we analysed a few simulations with different feedback channels turned on:

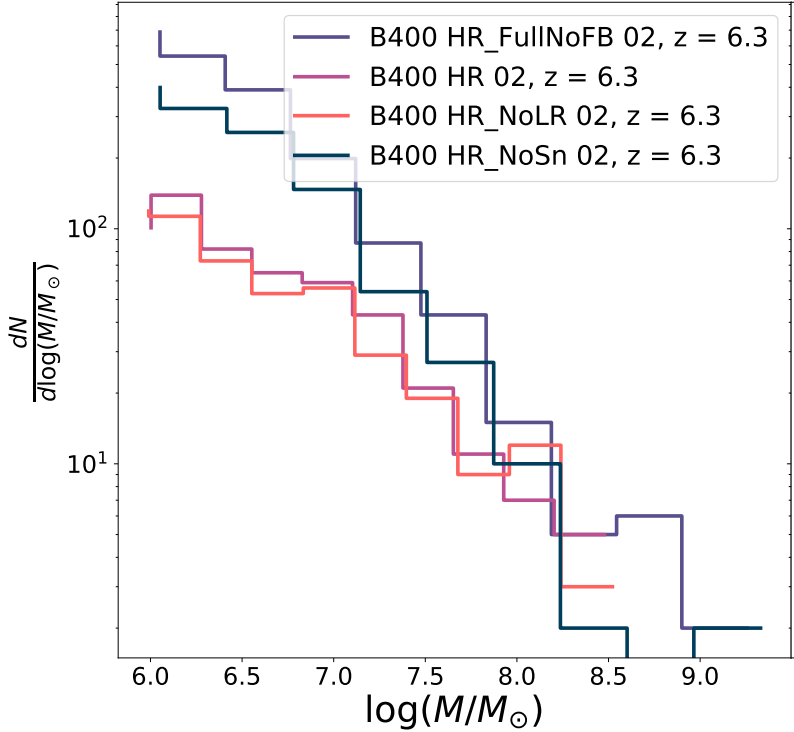


Figure 12: The mass function for B400-02 with different feedback channels turned on: no feedback, full physics, no long ranged radiative pressure and no supernovae feedback. Only clusters younger than 100 Myrs were considered.

		B400-10 HR			
Feedback model		Full Physics	No Feedback	No Long-Ranged	No Supernovae
$N_{\text{tot}}$		533	1977	486	1223
$\beta$		$1.6 \pm 0.1$	$1.9 \pm 0.1$	$1.6 \pm 0.1$	$1.8 \pm 0.1$

Table 3: The number of globular clusters per galaxy  $N_{\text{tot}}$  as well as the fitted slope  $\beta$  for four different feedback implementations in B400-10.

- Full physics: All feedback included (*FullPhys*)
- No long ranged radiation pressure (*NoLR*)
- No supernovae feedback (*NoSn*)
- All feedback turned off (*FullNoFB*)

Instead of re-simulating each galaxy with different feedback channels from scratch, the already available full-physics (galaxies we also used earlier) simulations were taken and re-simulated from about  $z = 7.4$  with the specific feedback channels. In order to properly compare the impact feedback has on globular clusters we need to only consider the clusters which formed after the switch in feedback models. Thus, we discarded all clusters older than 100 Myrs. Since the formation of a clusters is not a binary process, we needed to determine a point at which we considered a cluster 'born'. This point we chose to be after the cluster contained 50% of its final stellar mass.

The resulting mass functions can be seen in Figure 12. As we can see, there is almost no difference between *FullNoFB* and *NoSn* which suggests supernovae feedback to have the biggest impact on the mass function of globular clusters. Furthermore, *FullPhys* and

*NoLR* also look nearly identical, which leads us to believe that long ranged radiative pressure only affects the globular cluster mass function minimally. Table 3 we can see the corresponding slopes and cluster numbers for the different feedback models. Once again, there is a stark difference in both slope and number of clusters between *FullPhys/NoLR* and *FullNoFB/NoSn*

It seems that feedback does have a big impact on the number of clusters as well as their mass function. Mostly affected by feedback seem to be the low mass clusters, which are more prone to evaporation when energy is injected into the system through feedback.

#### 4.7 Where do the Globular Clusters form?

Finally, we were also interested in where globular clusters form and where they move over time. This question required us to run PHINDER on as many snapshots of the simulation as possible, in order to track the globular clusters. There is no way to definitively track a cluster over multiple snapshots, since PHINDER identifies clusters for each snapshot separately without having knowledge of the previous one. Thus, for each snapshot we used the age of the clusters as an indicator of where the clusters are located in different stages of their life. Once again, we defined the birth of a clusters to be after it contained 50% of its final mass. It is important to note, that *final* here means the mass of the cluster identified in snapshot  $X$  by PHINDER. Thus, if the cluster is detected again in snapshot  $X + 1$  and has gained mass, its birth time will be different compared to the previous snapshot. We tried to combat this ambiguity by using a discrete rather than continuous age classification.

The age and location of the clusters were all compiled into a movie, of which three frames can be seen in Figure 13. What could be seen in the movie, and is also apparent in the figure, is that the younger clusters (yellow in figure) tend to be located near denser stellar regions. The older (redder in figure) the clusters get, the more spread out they are around the galaxy. From the movie it can also be seen that a large amount of the clusters are accreted from outside the virial radius of the galaxy. This is not surprising at this stage since the galaxy is still forming and is frequently accreting smaller surrounding galaxies.

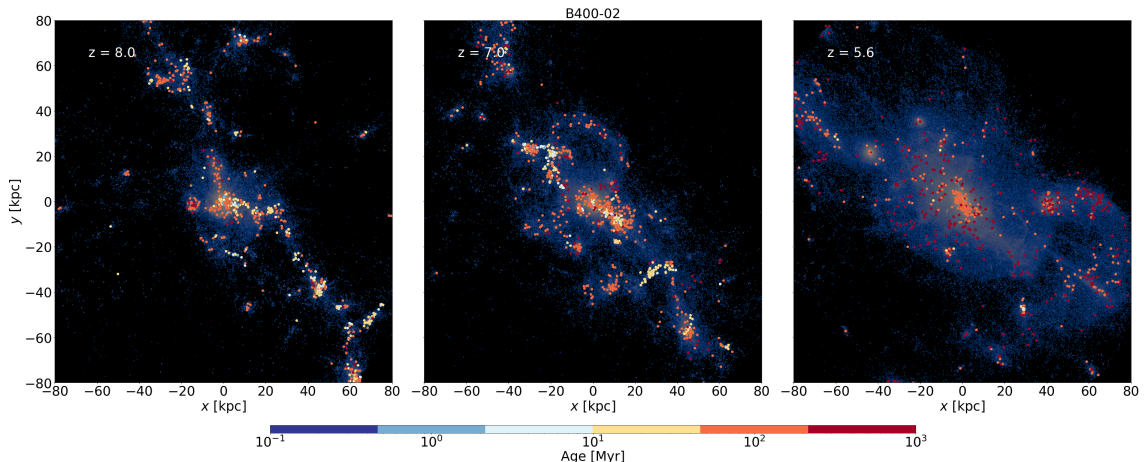


Figure 13: This figure depicts the stellar densities overlaid by the location of clusters at three different redshifts in galaxy B400-02. The colour of the cluster indicates its approximate age.

## 5 Conclusion

In this semester project we analysed globular clusters in high redshift galaxies using cosmological zoom-in simulations. The simulations were performed using the massively-parallel code GIZMO together with physics from the FIRE-2 project.

In a first step the globular clusters were identified using the python package PHINDER. Using the python visualisation package FIRE-Studio the luminosities of the globular clusters were calculated and thus also the cluster luminosity functions. It was found that instead of following a power law, the luminosity functions had a log-normal shape. Before drawing any conclusions from this result more investigation needs to be done, such as calculating the luminosities of the clusters from scratch.

Next, the cluster mass function was analysed. We found that the globular clusters follow a power-law shaped mass function, as expected. The values for the slopes  $\beta$  were always close to, but below, the expected value of 2. Up until this point all of the analysis was done on simulations with a fixed resolution. We wanted to test how our results are affected if we increase the resolution. Concerning the mass function, we found that a higher resolution merely added clusters in the previously undetected low-mass range. This left the shape of the mass function unchanged.

Another point of interest was how the number of clusters in a galaxy relates to its halo mass. We found that our HR data almost perfectly followed equation 8 from Burkert and Forbes 2020. Taking into account the appropriate mass range on the other hand, shifted our data points along the  $y$ -axis and no longer agree with the observational data. Among other things, this could be due to the redshift at which we are probing the clusters, or an error in how PHINDER identifies the clusters.

We also tested how different feedback models affect the mass function of the globular clusters. Feedback, especially supernovae feedback, seems to influence the number of low mass clusters. Having found this, it would be interesting to see how the implementation of active galactic nuclei (AGN) feedback would change our results.

Finally, we also took a look at where globular clusters form. We found that the clusters form in high density regions and subsequently become more dispersed. This agrees with the 2-phase model proposed by Kruijssen 2015.

Further investigation would include finding a second way to identify the clusters and comparing with the results from PHINDER as well as calculating the luminosity of the clusters from scratch. Considering how important feedback is, it will also be interesting to see how the next version of FIRE (FIRE-3), which includes AGN, will change the results found here.

## Acknowledgements

First of all I would like to thank Professor Robert Feldmann for giving me the opportunity to work on this project. I am also very thankful for the time he took out of his day for the weekly meetings as well as the freedom I was given to pursue ideas of my own.

I would also like to thank Professor Lavinia Heisenberg for supervision this project and meeting with us to discuss the progress I had made.

Finally, I would like to thank Dr. Luigi Bassini for being a great mentor and helping me navigate the details of this project. He was always quick to respond to any questions I had (and I always have many) and showed enthusiasm for any results which made the whole project feel more collaborative.

## Bibliography

- Burkert, Andreas and Duncan A. Forbes (Jan. 2020). “High-precision Dark Halo Virial Masses from Globular Cluster Numbers: Implications for Globular Cluster Formation and Galaxy Assembly”. In: *The Astronomical Journal* 159.2, p. 56. ISSN: 1538-3881. DOI: [10.3847/1538-3881/ab5b0e](https://doi.org/10.3847/1538-3881/ab5b0e). URL: <http://dx.doi.org/10.3847/1538-3881/ab5b0e>.
- Hopkins, Philip F et al. (June 2018). “FIRE-2 simulations: physics versus numerics in galaxy formation”. In: *Monthly Notices of the Royal Astronomical Society* 480.1, pp. 800–863. ISSN: 1365-2966. DOI: [10.1093/mnras/sty1690](https://doi.org/10.1093/mnras/sty1690). URL: <http://dx.doi.org/10.1093/mnras/sty1690>.
- Hopkins, Philip F. (Apr. 2015). “A new class of accurate, mesh-free hydrodynamic simulation methods”. In: *Monthly Notices of the Royal Astronomical Society* 450.1, pp. 53–110. ISSN: 1365-2966. DOI: [10.1093/mnras/stv195](https://doi.org/10.1093/mnras/stv195). URL: <http://dx.doi.org/10.1093/mnras/stv195>.
- Hopkins, Philip F. et al. (Nov. 2014). “Galaxies on FIRE (Feedback In Realistic Environments): stellar feedback explains cosmologically inefficient star formation”. In: 445.1, pp. 581–603. DOI: [10.1093/mnras/stu1738](https://doi.org/10.1093/mnras/stu1738). arXiv: [1311.2073 \[astro-ph.CO\]](https://arxiv.org/abs/1311.2073).
- Kruijssen, J. M. Diederik (Nov. 2012). “On the fraction of star formation occurring in bound stellar clusters”. In: 426.4, pp. 3008–3040. DOI: [10.1111/j.1365-2966.2012.21923.x](https://doi.org/10.1111/j.1365-2966.2012.21923.x). arXiv: [1208.2963 \[astro-ph.CO\]](https://arxiv.org/abs/1208.2963).
- (Oct. 2015). “Globular clusters as the relics of regular star formation in ‘normal’ high-redshift galaxies”. In: *Monthly Notices of the Royal Astronomical Society* 454.2, pp. 1658–1686. ISSN: 0035-8711. DOI: [10.1093/mnras/stv2026](https://doi.org/10.1093/mnras/stv2026). URL: <https://doi.org/10.1093/mnras/stv2026>.
- Ma, Xiangcheng et al. (Feb. 2020). “Self-consistent proto-globular cluster formation in cosmological simulations of high-redshift galaxies”. In: *Monthly Notices of the Royal Astronomical Society* 493.3, pp. 4315–4332. ISSN: 1365-2966. DOI: [10.1093/mnras/staa527](https://doi.org/10.1093/mnras/staa527). URL: <http://dx.doi.org/10.1093/mnras/staa527>.
- NASA, ESA, and A. Feild(STScl) (2019). “Globular Clusters Around Milky Way”. In: URL: <https://hubblesite.org/contents/media/images/2019/16/4369-Image.html?keyword=Globular%20Clusters>.
- Portegies Zwart, Simon F., Stephen L.W. McMillan, and Mark Gieles (Aug. 2010). “Young Massive Star Clusters”. In: *Annual Review of Astronomy and Astrophysics* 48.1, pp. 431–493. ISSN: 1545-4282. DOI: [10.1146/annurev-astro-081309-130834](https://doi.org/10.1146/annurev-astro-081309-130834). URL: <http://dx.doi.org/10.1146/annurev-astro-081309-130834>.

- Schechter, P. (Jan. 1976). “An analytic expression for the luminosity function for galaxies.” In: *The Astronomical Journal* 203, pp. 297–306. DOI: [10.1086/154079](https://doi.org/10.1086/154079).
- Spitler, Lee R., Duncan A. Forbes, and Michael A. Beasley (Sept. 2008). “Extending the baseline: Spitzer mid-infrared photometry of globular cluster systems in the Centaurus A and Sombrero Galaxies”. In: *Monthly Notices of the Royal Astronomical Society* 389.3, pp. 1150–1162. ISSN: 0035-8711. DOI: [10.1111/j.1365-2966.2008.13681.x](https://doi.org/10.1111/j.1365-2966.2008.13681.x). eprint: <https://academic.oup.com/mnras/article-pdf/389/3/1150/3324128/mnras0389-1150.pdf>. URL: <https://doi.org/10.1111/j.1365-2966.2008.13681.x>.
- Springel, Volker, Naoki Yoshida, and Simon D.M. White (Apr. 2001). “GADGET: a code for collisionless and gasdynamical cosmological simulations”. In: *New Astronomy* 6.2, pp. 79–117. ISSN: 1384-1076. DOI: [10.1016/s1384-1076\(01\)00042-2](https://doi.org/10.1016/s1384-1076(01)00042-2). URL: [http://dx.doi.org/10.1016/S1384-1076\(01\)00042-2](http://dx.doi.org/10.1016/S1384-1076(01)00042-2).
- Whitmore, Bradley C. et al. (Oct. 1999). “The Luminosity Function of Young Star Clusters in “the Antennae” Galaxies (NGC 4038/4039)”. In: *The Astronomical Journal* 118.4, pp. 1551–1576. ISSN: 0004-6256. DOI: [10.1086/301041](https://doi.org/10.1086/301041). URL: <http://dx.doi.org/10.1086/301041>.